PCCP

Cite this: *Phys. Chem. Chem. Phys.*, 2015, **17**, 31188

Engineering oxygen vacancies towards self-activated BaLuAl$_x$Zn$_{4-x}$O$_{7-(1-x)/2}$ photoluminescent materials: an experimental and theoretical analysis†

Lan Ma,[a] Zhiguo Xia,*[a] Victor Atuchin,[bcd] Maxim Molokeev,[ef] S. Auluck,[gh] A. H. Reshak[ij] and Quanlin Liu[a]

Novel self-activated yellow-emitting BaLuAl$_x$Zn$_{4-x}$O$_{7-(1-x)/2}$ photoluminescent materials were investigated by a combined experimental and theoretical analysis. The effects of Al/Zn composition modulation, calcination atmosphere and temperature on the crystal structure and photoluminescence properties have been studied *via* engineering oxygen vacancies. Accordingly, BaLuAl$_{0.91}$Zn$_{3.09}$O$_7$ prepared in an air atmosphere was found to be the stable crystalline phase with optimal oxygen content and gave a broad yellow emission band with a maximum at 528 nm. The self-activated luminescence mechanism is ascribed to the O-vacancies based on the density functional theory (DFT) calculation. A theoretical model originating from the designed oxygen vacancies has been proposed in order to determine the influence of O-vacancies on the band structure and self-activated luminescence. Therefore, the appearance of a new local energy level in the band gap will cause the wide-band optical transitions in the studied BaLuAl$_x$Zn$_{4-x}$O$_{7-(1-x)/2}$ materials.

[a] *School of Materials Sciences and Engineering, University of Science and Technology Beijing, Beijing 100083, China. E-mail: xiazg@ustb.edu.cn; Fax: +86-10-82377955; Tel: +86-10-82377955*

[b] *Laboratory of Optical Materials and Structures, Institute of Semiconductor Physics, SB RAS, Novosibirsk 630090, Russia*

[c] *Functional Electronics Laboratory, Tomsk State University, Tomsk 634050, Russia*

[d] *Laboratory of Semiconductor and Dielectric Materials, Novosibirsk State University, Novosibirsk 630090, Russia*

[e] *Laboratory of Crystal Physics, Kirensky Institute of Physics, SB RAS, Krasnoyarsk 660036, Russia*

[f] *Department of Physics, Far Eastern State Transport University, Khabarovsk 680021, Russia*

[g] *Council of Scientific and Industrial Research – National Physical Laboratory Dr K S Krishnan Marg, New Delhi 110012, India*

[h] *Department of Physics, Indian Institute of Technology, Hauz Khas, New Delhi 110016, India*

[i] *New Technologies – Research Centre, University of West Bohemia, Univerzitni 8, 306 14 Pilsen, Czech Republic*

[j] *Center of Excellence Geopolymer and Green Technology, School of Material Engineering, University Malaysia Perlis, 01007 Kangar, Perlis, Malaysia*

† Electronic supplementary information (ESI) available. See DOI: 10.1039/c5cp05130d

1 Introduction

Rare earth doped photoluminescent materials have been extensively developed in recent years and applied to many optical materials fields, such as white light-emitting diodes (WLEDs), solar spectral converters and advanced photoelectron devices, and so on.[1–4] Although rare earth ions play an important role in the fabrication of new photoluminescent materials, the limited rare earth resources encourage researchers to investigate new rare earth-free luminescent materials for different optical applications.[5–8] The spectroscopic properties of the self-activated phosphors are generally governed by the optical transitions through the oxygen-vacancy-related states in the band gap, so that their excitation and emission spectra are strongly dependent on the chemical composition, intrinsic structural properties and different preparation conditions.[9–12]

A kind of LnBaZn$_3$AlO$_7$ (Ln = Lu, Sm) compound with the general structural type "1147" was firstly reported in 1996. The structure is partly disordered and two mixed cation positions were found with different Zn/Al ratios.[13,14] As we know, the structural disorder is a positive factor for the creation of wide-emission-band phosphors in the doped systems.[15–17] More recently, the evaluation of the "1147" systems was continued and now the general formula can be written as LnBaM$_4$O$_7$ (Ln = rare earth and Ca; M = Co, Fe, Mn, Zn, Ga, and Al).[18–20] Several rare-earth-containing phosphors were proposed from the LnBaM$_4$O$_7$-type hosts when M = Zn or Ga.[21–23] Up to now, however, self-activated luminescence remained unknown in this kind of complex oxide system. In this paper, novel self-activated yellow-emitting BaLuAl$_x$Zn$_{4-x}$O$_{7-(1-x)/2}$ photoluminescent materials are reported, and their structural and luminescence properties were comparatively evaluated based on different chemical compositions and synthesis atmospheres. A theoretical model originating from the designed oxygen vacancies has been proposed, and it is found that the self-activated luminescence is ascribed to the appearance of a new local energy level band induced by the oxygen-vacancy-related states in the band gap.

2 Experimental section

2.1 Materials and synthesis

According to the selected compositions of $BaLuAlZn_3O_7$, $BaLuAl_{0.91}Zn_{3.09}O_7$ and $BaLuAl_{0.8}Zn_{3.2}O_7$, the designed samples were prepared by the high temperature solid-state reaction. The raw materials of $BaCO_3$ (AR), Lu_2O_3 (99.99%), Al_2O_3 (AR) and ZnO (AR) were mixed in an agate mortar. Then, the mixtures were placed in alumina crucibles and sintered at several selected temperatures from 1300 °C to 1500 °C and different atmospheres, air, Ar and 95%N_2/5%H_2. After cooling down naturally, the fired samples were ground and prepared for measurements.

2.2 Structural and optical characterization

The powder diffraction data were obtained by X-ray powder diffraction using a Philips X'Pert PW-3040 device (Cu Kα radiation, 40 kV, 35 mA). The Rietveld refinement was performed using package TOPAS 4.2. Photoluminescence spectra were measured using a fluorescence spectrophotometer (F-4600, HITACHI, Japan) with a 150 W xenon lamp as the light source. The luminescence decay curves were obtained using a FLSP9200 fluorescence spectrophotometer (Edinburgh Instruments Ltd, UK). Diffuse reflection spectra were measured on a UV-Vis-NIR spectrophotometer (SHIMADZU UV-3600) attached with an integrating sphere. $BaSO_4$ was used as a reference standard. High-resolution transmission electron microscopy (HRTEM) images were obtained using a JEM-2011 microscope (JEOL, Japan), which is equipped with an energy dispersive X-ray spectrometer (EDS, INCA, Oxford instruments, UK).

2.3 Calculation methodology

The band structure calculations were performed based on the X-ray crystallographic data of $BaLuAl_{0.91}Zn_{3.09}O_7$ obtained in the present study. The positions of the atoms were relaxed so as to minimize the forces on the atoms. We have used the generalized gradient approximation (PBE-GGA)[24] within the full potential linear augmented plane wave (FPLAPW+lo) method as embodied in the WIEN2k code.[25] The resulting relaxed geometry was used to calculate the electronic structure and, hence, the associated properties using PBE-GGA and the recently modified Becke–Johnson potential (mBJ).[26] The muffin-tin radii (R_{MT}) of the atoms were chosen in such a way that the spheres did not overlap. The value of R_{MT} is taken to be 2.19 a.u. (Ba), 2.15 a.u. (Lu), 1.92 a.u. (Zn) and 1.59 a.u. for Al and O. To achieve the total energy convergence, the basis functions in the interstitial region (IR) were expanded up to $R_{MT} \times K_{max} = 7.0$ and inside the atomic spheres for the wave function. The maximum value of l was taken as $l_{max} = 10$, while the charge density is Fourier expanded up to $G_{max} = 12$ $(a.u.)^{-1}$. Self-consistency is obtained using 300 k points in the irreducible Brillouin zone (IBZ). The self-consistent calculations are converged since the total energy of the system is stable within 0.00001 Ry. The electronic properties are calculated using 970 k points in the IBZ. The details of DFT calculations and level of theory are also given in the ESI.†

3 Results and discussion

Discovery of the new self-activated photoluminescent materials is the main topic of the present study. Only the $BaLuAl_{0.91}Zn_{3.09}O_7$ phase can be identified from the general structural type "1147" in the Inorganic Crystal Structure Database (ICSD) when the chemical elements Ba, Lu, Al, Zn and O have been selected. As reported by Rabbow, when they tried to prepare $BaLuAlZn_3O_7$, which is isotypic to $Ba_2Ln_2Zn_8O_{13}$ in spite of a small difference in the oxygen content, the $BaLuAl_{0.91}Zn_{3.09}O_7$ phase can only be found and the crystal structure has been determined from the single crystal data. After a careful comparison, it is found that the crystal structure of $BaLuAlZn_3O_7$ without vacancies (Fig. 1a) can be considered as a parent phase of the defect $BaLuAl_xZn_{4-x}O_{7-(1-x)/2}$ structure (Fig. 1b). Some Al^{3+} ions in this parent phase can be substituted by Zn^{2+} ions, in this case, the unit cell charge becomes negative and charge compensation is required. Only O^{2-} ion loss can provide the zero charge balance and a defect structure is formed according to the schema $2Al^{3+} + O^{2-} = 2Zn^{2+}$ (Fig. 1). Therefore, we believed that the experimental conditions, such as sintering atmospheres, Al/Zn ratios, and reaction temperature, would be very important for the phase formation and possible self-activated luminescence in such a defect system.

Since we can only find the standard data of the $BaLuAl_{0.91}Zn_{3.09}O_7$ phase from the Joint Committee on Powder Diffraction Standards (JCPDS) and the ICSD files, we have firstly prepared the $BaLuAl_{0.91}Zn_{3.09}O_7$ phase in different atmospheres. As shown in Fig. S1 in the ESI,† the XRD patterns of the nominal $BaLuAl_{0.91}Zn_{3.09}O_7$

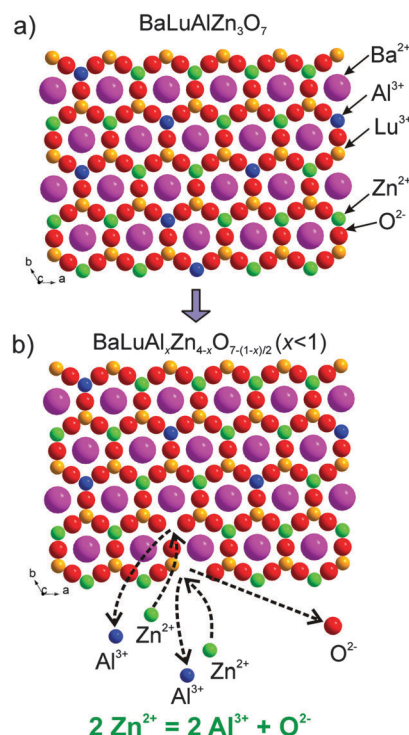**Fig. 1** Mechanism of O^{2-} vacancy formation using parent phase $BaLuAlZn_3O_7$ (a) which undergoes $2Al^{3+} \rightarrow 2Zn^{2+}$ substitution and O^{2-} loss resulting in the $BaLuAl_xZn_{4-x}O_{7-(1-x)/2}$ defect structure (b), with $x < 1$.

This journal is © the Owner Societies 2015

Phys. Chem. Chem. Phys., 2015, **17**, 31188–31194 | **31189**

composition prepared in different atmospheres are compared at the same sintering temperature (1500 °C), and nearly pure $BaLuAl_{0.91}Zn_{3.09}O_7$ phases can be obtained in the air and inert Argon (Ar) atmosphere. In order to clarify the phase compositions of the as-prepared samples in different atmospheres, Fig. S2 (ESI†) shows the compared Rietveld plots of $BaLuAl_{0.91}Zn_{3.09}O_7$ prepared in air (a), Ar (b), and 95%N_2–5%H_2 (c) atmospheres. It is found that the main phase of $BaLuAl_{0.91}Zn_{3.09}O_7$ (96.7%) can be found for the sample prepared in air, and some minor impurity of ZnO (1.8%) and Lu_2O_3 (1.5%) can be also checked. As a comparison, we cannot get the $BaLuAl_{0.91}Zn_{3.09}O_7$ phase if the samples are prepared in a N_2–H_2 reducing atmosphere, and Lu_2O_3 and $BaAl_2O_4$ act as the main phases. Although the sample prepared in an Ar atmosphere can also get the nearly pure phase, only the $BaLuAl_{0.91}Zn_{3.09}O_7$ phase prepared in the air atmosphere can show the luminescence under the ultraviolet light excitation, as given in the photoluminescence and emission spectra shown in Fig. S3 (ESI†). We believe that the air atmosphere in the phase formation plays an important role in the optimal oxygen vacancy quantity and the induced photoluminescence, and the related mechanism will be discussed later. Therefore, an air atmosphere is selected in the following experiment aimed at the preparation of the $BaLuAl_{0.91}Zn_{3.09}O_7$-based phase.

Since the Al/Zn ratio also affects the phase structure of the $BaLu(Al,Zn)_4O_7$ compound, it may produce an important influence on the photoluminescence behaviour. Therefore, three kinds of $BaLu(Al,Zn)_4O_7$ compounds with different Al/Zn ratios, $BaLuAlZn_3O_7$, $BaLuAl_{0.91}Zn_{3.09}O_7$ and $BaLuAl_{0.8}Zn_{3.2}O_7$, have been prepared based on their corresponding nominal chemical compositions. As given in Fig. S4 (ESI†), the as-prepared $BaLuAlZn_3O_7$, $BaLuAl_{0.91}Zn_{3.09}O_7$ and $BaLuAl_{0.8}Zn_{3.2}O_7$ samples belong to the same phase, and the XRD patterns of them agree well with the standard data of $BaLuAl_{0.91}Zn_{3.09}O_7$ (JCPDS, 85-0252). Furthermore, the Rietveld plots of the three samples are given in Fig. 2, and the refinement results also verified that they belong to the same phases depending on different Al/Zn ratios. Accordingly, Fig. 3 shows the bond valence sums for each ion in the compounds: (a) $BaLuAlZn_3O_7$; (b) $BaLuAl_{0.91}Zn_{3.09}O_7$ and (c) $BaLuAl_{0.8}Zn_{3.2}O_7$. The similarity of the ion bond valence values, which were calculated using bond lengths, for all presented compounds proves that the crystal structures are very close to each other. Therefore, the substitution $2Al^{3+} + O^{2-} \rightarrow 2Zn^{2+}$ will not lead to noticeable ion shifts, and, as a consequence, any differences in physical properties should be accounted by the ion occupancy change. It should be noted that BVS values calculated for O1 and O3 ions are in the range of $-(1.760–1.814)$. However, the O2 ion has noticeably higher BVS values in the range of $-(1.921–1.965)$. Such a situation can be realized in the case when O^{2-} vacancies appear mainly in O1 and O3 sites instead of the O2 site. The linear cell volume increases upon increasing average ion radius IR(Al/Zn) in the $BaLuAl_xZn_{3-x}O_7$ compounds (Fig. 3d) proving that the suggested Al/Zn ratios obtained for $BaLuAlZn_3O_7$, $BaLuAl_{0.91}Zn_{3.09}O_7$ and $BaLuAl_{0.8}Zn_{3.2}O_7$ are close to real ones. Using general formula $BaLuAl_xZn_{4-x}O_{7-(1-x)/2}$ one can rewrite chemical formulas of these compounds as $BaLuAlZn_3O_7$, $BaLuAl_{0.91}Zn_{3.09}O_{6.955}$ and $BaLuAl_{0.8}Zn_{3.2}O_{6.9}$, and it is evident that O^{2-} defect concentration

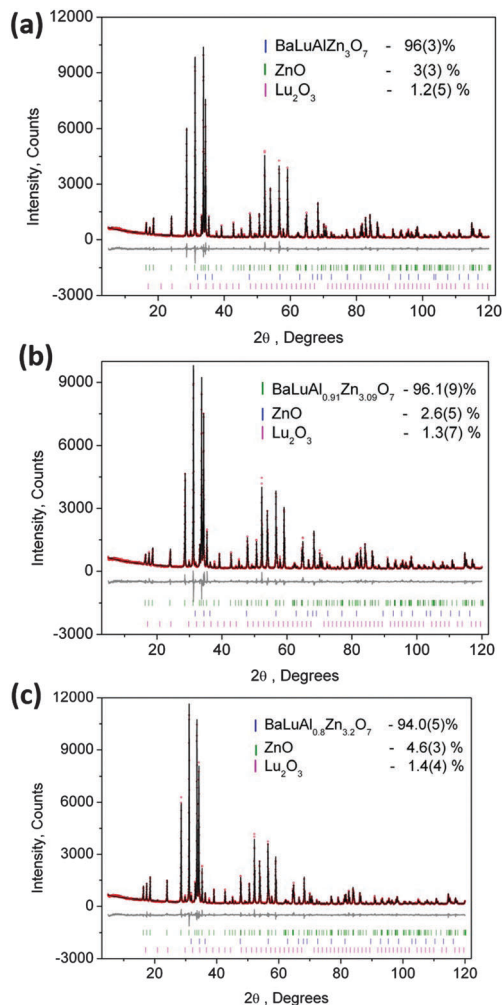Fig. 2 Difference Rietveld plots of $BaLuAl_{0.91}Zn_{3.09}O_7$-type phases formed at different Al/Zn ratios, (a) Al/Zn = 1 : 3, (b) Al/Zn = 0.91/3.09, and (c) Al/Zn = 0.8/3.2.

increases in these compounds, respectively. Therefore, a noticeable luminescence effect can be expected mainly for the compounds $BaLuAl_{0.91}Zn_{3.09}O_{6.955}$ and $BaLuAl_{0.8}Zn_{3.2}O_{6.9}$. As far as the concentration of O^{2-} vacancies for both of them is close, they can show similar properties, but markedly differ from those of $BaLuAlZn_3O_7$.

Although the structures of $BaLu(Al,Zn)_4O_7$ compounds at different Al/Zn ratios are nearly invariable, $BaLuAl_{0.91}Zn_{3.09}O_7$ has the optimal self-activated photoluminescence properties, and the emission intensity of this sample is the highest one among these series of samples, as given in Fig. S5 (ESI†). Accordingly, the chemical composition of $BaLuAl_{0.91}Zn_{3.09}O_7$ is selected in the following discussion. The XRD patterns recorded from the $BaLuAl_{0.91}Zn_{3.09}O_7$ samples prepared at different temperatures are shown in Fig. S6 (ESI†). When the annealing temperature is below 1200 °C or as high as 1580 °C, the Lu_2O_3 impurity was obviously observed. At $1200 < T < 1580$ °C, the measured XRD patterns are free of foreign components and match well with the known $BaLuAl_{0.91}Zn_{3.09}O_7$ pattern (PDF Card no. 85-0252).[13] Moreover, we have also
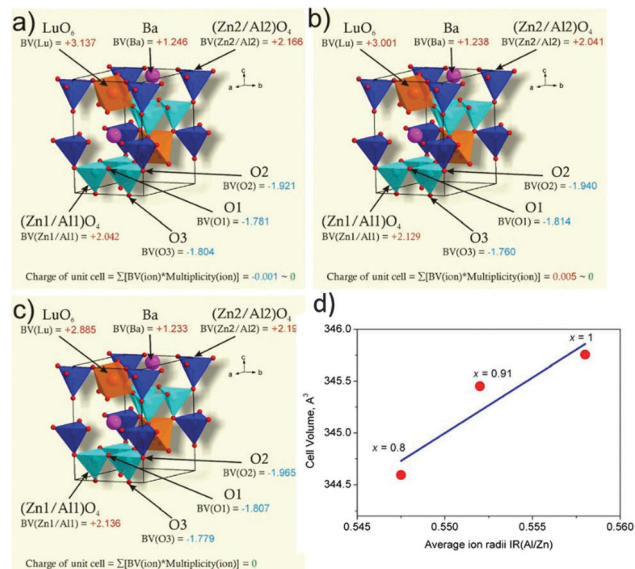
Fig. 3 Bond valence sums for each ion in: (a) $BaLuAlZn_3O_7$, (b) $BaLuAl_{0.91}Zn_{3.09}O_7$, and (c) $BaLuAl_{0.8}Zn_{3.2}O_7$, and (d) linear increase of cell volume per average ion radius IR(Al/Zn) of compounds $BaLuAl_xZn_{3-x}O_7$.

compared the photoluminescence properties of $BaLuAl_{0.91}Zn_{3.09}O_7$ phosphors prepared at different annealing temperatures. As shown in Fig. S7 (ESI†), the sample prepared at 1500 °C possesses the strongest emission intensity, suggesting that such an experimental condition is the best one. Based on the above discussions, we can optimize the chemical composition and synthesis conditions for the self-activated $BaLuAl_xZn_{4-x}O_{7-(1-x)/2}$ photoluminescent materials, and the optimum photoluminescence properties can be realized with chemical composition of $BaLuAl_{0.91}Zn_{3.09}O_7$ prepared in the air at 1500 °C.

The morphological structures and chemical composition of the optimized $BaLuAl_{0.91}Zn_{3.09}O_7$ sample have been checked by transmission electron microscopy (TEM) and scanning electron microscopy (SEM), respectively. Fig. 4a presents the TEM image of the selected particle, and the size is approximately 200 nm. In order to show the overall morphologies, Fig. 4b presents the SEM image of the selected $BaLuAl_{0.91}Zn_{3.09}O_7$ sample. From the observed SEM image, we can find that the morphologies are irregular and the size is not homogeneous in the range of 1–20 μm. Additionally, the sample for quantitative composition analysis of elemental composition was performed by ICP-OES, and the weight percentages of Ba: 19.64%, Lu: 25.25%, Al: 3.55%, Zn: 32.69% and
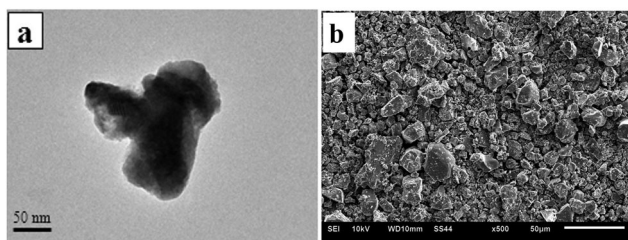

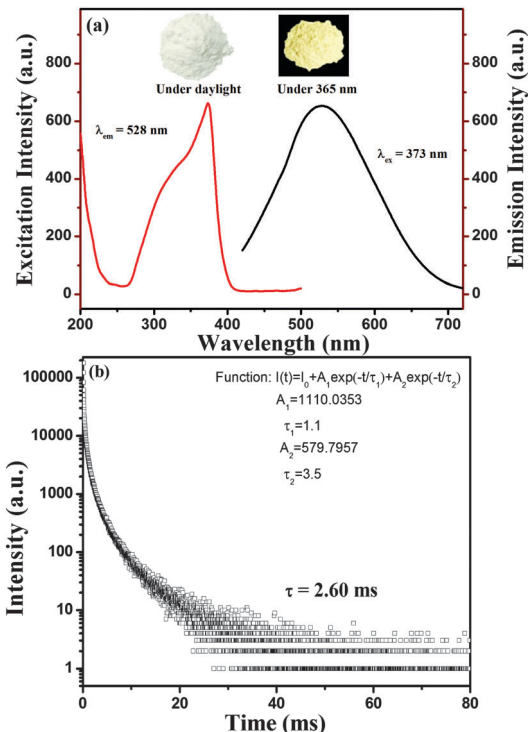**Fig. 4** TEM image (a) and SEM image (b) of the selected $BaLuAl_{0.91}Zn_{3.09}O_7$ sample.

Fig. 5 (a) PLE and PL spectra of the optimized $BaLuAl_{0.91}Zn_{3.09}O_7$ photoluminescent material, and the digital photographs of the phosphor under daylight and a 365 nm UV lamp (inset); (b) decay curve monitored at 528 nm upon excitation of 373 nm for as-prepared $BaLuAl_{0.91}Zn_{3.09}O_7$ phosphor.

O: 19.15% are very close to the calculated nominal values. Also, the low oxygen content was detected in the samples, and the lack of oxygen supported the existence of oxygen vacancies, which will be discussed later.

The photoluminescence excitation and emission spectra of optimized $BaLuAl_{0.91}Zn_{3.09}O_7$ phosphors are shown in Fig. 5a. The excitation spectra consist of a broad band covering the spectral range of 270–400 nm with an abrupt edge at $\sim$400 nm. The broad absorption band possesses the narrow maximum at 373 nm and the shoulder at $\sim$333 nm. Besides this band, the absorption increases at <240 nm. As for photoemission from the $BaLuAl_{0.91}Zn_{3.09}O_7$ powder upon UV excitation (373 nm), the broad band ranging from 420 nm to 720 nm with the shallow maximum at 528 nm is observed. As shown in the inset in Fig. 5a by the digital photo, the $BaLuAl_{0.91}Zn_{3.09}O_7$ powder excited at 373 nm is of yellow color. To estimate the luminescence lifetime for the sample, the decay curve was measured under 373 nm UV excitation, as shown in Fig. 5b. The decay curve can be well fitted by the biexponential function:[2]

$$I(t) = I_0 + A_1 \exp(-t/\tau_1) + A_2 \exp(-t/\tau_2) \qquad (1)$$

where I and I_0 are the phosphorescence intensities at time t and 0, A_1 and A_2 are constants, and τ_1 and τ_2 are rapid and slow lifetimes in the exponential components, respectively. The effective lifetime constant τ can be calculated according to the following equation:[2]

This journal is © the Owner Societies 2015

Phys. Chem. Chem. Phys., 2015, **17**, 31188–31194 | **31191**

$$\tau = (A_1\tau_1^2 + A_2\tau_2^2)/(A_1\tau_1 + A_2\tau_2) \qquad (2)$$

Based on the above data and eqn (1) and (2), the values of A_1, A_2, τ_1, and τ_2 are 1110.04, 579.80, 1.10 and 3.50, respectively. As we know, the lifetime value gives the total decay rate (radiative plus nonradiative rates). The physical origin of different decay components means the lifetime of the different luminescence centers, and we can find that there is little difference for the decay component, 1.1 ms and 3.5 ms, which means that they belong to the same kind of emission center. Therefore, the average decay time value of $BaLuAl_{0.91}Zn_{3.09}O_7$ was calculated to be ~2.60 ms, therefore, such a long lifetime value is generally related to the defect luminescence. Such a value is also of the same order of magnitude as the other self-activated phosphors, such as $Li_2Ca_2ScV_3O_{12}$.[27]

To consider the possible mechanism of the self-activated luminescence and the corresponding optical transitions, it is needed to reveal the band structure of the compound. The relaxed unit cell of $BaLuAl_{0.91}Zn_{3.09}O_7$ is presented in Fig. S8(a) (ESI†). In addition, we have performed calculations for $BaLuAl_{0.91}Zn_{3.09}O_7$ modified by removing two oxygen atoms in the vicinity of Zn and Al atoms, to form a pair of oxygen vacancies and seek the influence on the band structure and self-activated luminescence. Therefore, the chemical formula of the resulting compound with vacancies is $BaLuAl_{0.91}Zn_{3.09}O_6$. The crystal structure of $BaLuAl_{0.91}Zn_{3.09}O_6$ is illustrated in Fig. S8(b) (ESI†) where the oxygen vacancies are clearly shown. The electronic band structure along the high symmetry points of the first BZ and the angular momentum resolved projected density of states (PDOS) of oxygen atoms of $BaLuAl_{0.91}Zn_{3.09}O_7$ and $BaLuAl_{0.91}Zn_{3.09}O_6$ crystals are comparatively shown in Fig. 6. For simplicity we will call them as case1 for $BaLuAl_{0.91}Zn_{3.09}O_7$ and case2 for $BaLuAl_{0.91}Zn_{3.09}O_6$.

It has been found that the valence band maximum (VBM) for $BaLuAl_{0.91}Zn_{3.09}O_7$ is located at the M point of the BZ and the conduction band minimum (CBM) is located at the Γ point of the BZ, resulting in an indirect energy band gap of 1.438 eV (PBE-GGA) and 3.135 eV (mBJ). It is clear that mBJ succeeds by a large amount in bringing the calculated energy gap in close agreement with the measured value of 3.16 eV. Whereas $BaLuAl_{0.91}Zn_{3.09}O_6$ exhibits a direct band gap (M–M) of about 1.335 eV (PBE-GGA) and 2.689 eV (mBJ). Therefore, in the following, we show only the results obtained by mBJ. The PDOS shows the influence of the oxygen vacancies on the band dispersion. It is clear that in the VB of $BaLuAl_{0.91}Zn_{3.09}O_7$, there is a high density state region situated between −2.0 eV and the Fermi level (E_F) which belongs to the two O atoms (Fig. 6a), and this feature vanishes from the electronic band structure of $BaLuAl_{0.91}Zn_{3.09}O_6$ (Fig. 6b) due to the pair of oxygen vacancies. In Fig. S9(a and b) (ESI†) the total density of states along with the PDOS of the Lu atom is shown for both cases. The pair of oxygen vacancies significantly influences the TDOS. From the PDOS, it has been noticed that for case 1 the VBM is mainly formed by Zn, O1 and O3 atoms while for case 2 it is clear that these bands are vanished confirming the two oxygen vacancies keeping the VBM with a small contribution from O1 and O2. It is interesting to mention that there is a new local energy level appeared directly above E_F in the forbidden gap, which is composed of O-2p states. The appearance of this new band may cause the appearance of a new excitation band. Recently, Ding et al.[9] reported that the position of such a local energy level is changed due to the variation of oxygen vacancy concentration. Fig. S9(c) and (d) (ESI†) show the contribution of Zn and Ba atoms. It is clear that the O vacancies push Zn states which are situated at the VBM towards lower energies by around 2.0 eV, and this also leads to the Ba contribution reduction of around −9.0 and +12.0 eV. The contribution of the Al atom is illustrated in Fig. S9(e) and (f) (ESI†), which shows that the CBs of case 2 shift towards higher energies and form the CBM along with O1 and O2 atoms.

To verify the theoretical model mentioned above, the band gap of $BaLuAl_{0.91}Zn_{3.09}O_7$ was obtained by optical measurements and further discussed based on the above band structure calculation. The absorption spectrum of $BaLuAl_{0.91}Zn_{3.09}O_7$ phosphor is shown in the inset of Fig. 7a and such a spectrum
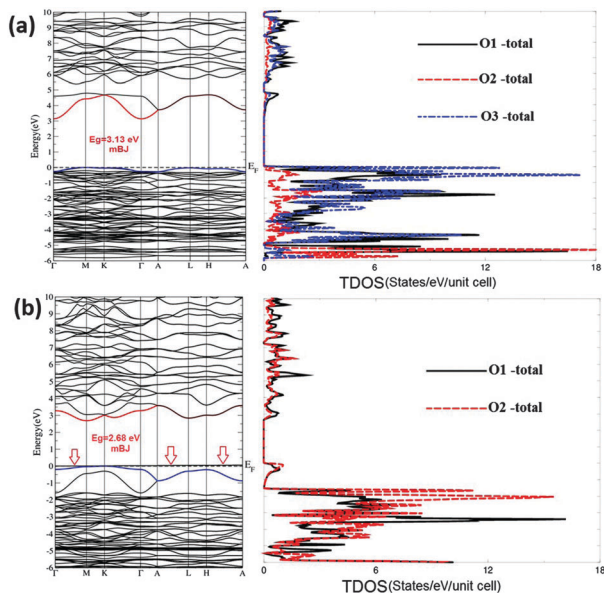

Fig. 6 The band gap structures for stoichiometric $BaLuAl_{0.91}Zn_{3.09}O_7$ (a) and defected $BaLuAl_{0.91}Zn_{3.09}O_6$ phase (b).
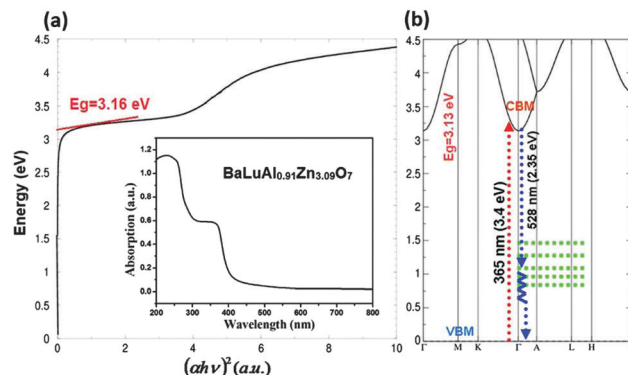

Fig. 7 (a) The band gap estimation of $BaLuAl_{0.91}Zn_{3.09}O_7$ phosphor, and the measured absorption spectra are shown in the inset. (b) Configuration diagram of the optical transitions inspired the $BaLuAl_{0.91}Zn_{3.09}O_7$ emission at ~528 nm. The oxygen-vacancy-related states in the gap are shown in green color.

can be further transferred into the energy scale according to the following equation:[28]

$$[F(R_\infty)h\nu]^n = A(h\nu - E_g) \qquad (3)$$

where $h\nu$ is the photon energy, E_g is the value of the band gap, A is a proportional constant, $n = 2$ for a direct transition or $1/2$ for an indirect transition, and $F(R_\infty)$ is a Kubelka–Munk function defined by the following equation:

$$F(R_\infty) = \frac{K}{S} = \frac{(1 - R)^2}{2R} \qquad (4)$$

where K represents the absorption coefficient, S represents the scattering coefficient, and R represents the reflectivity. Based on the above measured absorption spectrum and eqn (3) and (4), the optical band gap obtained for $BaLuAl_{0.91}Zn_{3.09}O_7$ is about 3.16 eV (392 nm), as shown in Fig. 7a. It should be pointed out that the optical absorption edge at 392 nm is in good relation with the excitation edge obtained at ~ 400 nm (Fig. 5(a)). Furthermore, there is no absorption over the photon energy below ~ 3.1 eV. The strong absorption increase, however, is evident at photon energy > 3.1 eV.

As also given in Fig. 7b, the band calculations in $BaLuAl_{0.91}Zn_{3.09}O_6$ exhibited the new state generation in the forbidden band gap due to oxygen vacancy introduction. Evidently, the different vacancy complexes may be constructed in this disordered structure and the vacancy-related states may be widely distributed in energy within the band gap. Then, the electrons excited to the conduction band by the UV illumination can emit the energy by the radiative transitions to oxygen-vacancy-related states over the band gap. The transitions are different in photon energy and this is the source of wide self-activated emission band detected in $BaLuAl_{0.91}Zn_{3.09}O_7$.

4 Conclusions

Novel self-activated yellow-emitting $BaLuAl_xZn_{4-x}O_{7-(1-x)/2}$ photoluminescent materials were investigated from a combined experimental and theoretical analysis. The effects of Al/Zn composition modulation and calcination atmosphere on the phase compositions of photoluminescence properties have been studied. The results show that the O-vacancies are the significant factor for the luminescence properties. DFT band calculations based on the compared results on $BaLuAl_{0.91}Zn_{3.09}O_6$ and $BaLuAl_{0.91}Zn_{3.09}O_7$ showed the new state generation in the forbidden band due to the fact that oxygen vacancy introduction plays an important role in the self-activated luminescence. Different vacancy complexes may be constructed in this disordered structure and the vacancy-related states may be widely distributed in energy within the band gap. Then, the electrons excited to the conduction band by the UV illumination can emit the energy by the radiative transition to oxygen-vacancy-related states over the band gap. The transitions are different in photon energy and this is the source of wide self-activated emission band detected in $BaLuAl_{0.91}Zn_{3.09}O_7$. Our findings on the oxygen vacancy-related photoluminescence based on the experimental data and the theoretical model will open up a suitable avenue to explore new self-activated photoluminescent materials. Thus, it is also topical to search for new compounds with general composition $BaLnAl_xZn_{4-x}O_{7-(1-x)/2}$, and compare their structural and spectroscopic properties for different rare-earth (Ln) elements.

Notes and references

1 G. Blasse and B. C. Grabmaier, *Luminescent Materials*, Springer Verlag, Berlin, 1994.
2 Z. G. Xia, C. G. Ma, M. S. Molokeev, Q. L. Liu, K. Rickert and K. R. Poeppelmeier, *J. Am. Chem. Soc.*, 2015, **13**, 12494.
3 Z. G. Xia, Y. Y. Zhang, M. S. Molokeev, V. V. Atuchin and Y. Luo, *Sci. Rep.*, 2013, **3**, 3310.
4 Y. Luo and Z. G. Xia, *J. Phys. Chem. C*, 2014, **118**, 23297.
5 C. M. Zhang and J. Lin, *Chem. Soc. Rev.*, 2012, **41**, 7938.
6 H. T. Li, Z. H. Kang, Y. Liu and S. T. Lee, *J. Mater. Chem.*, 2012, **22**, 24230.
7 Y. Guan, L. Qin, Y. L. Huang, C. X. Qin, D. L Wei and H. J. Seo, *Mater. Res. Bull.*, 2014, **54**, 24.
8 Y. F. Pu, Y. L. Huang, T. J. Tsuboi, W. Huang, C. L. Chen and H. J. Seo, *Mater. Lett.*, 2015, **149**, 89.
9 B. F. Ding, H. J. Qian, C. Han, J. Y. Zhang, S. E. Lindquist, B. Wei and Z. L. Tang, *J. Phys. Chem. C*, 2014, **118**, 25633.
10 J. Ren, X. Q. Xu, H. D. Zeng, G. R. Chen, D. Kong, C. J. Gu, C. M. Chen, Z. B. Liu and L. R. Kong, *J. Am. Ceram. Soc.*, 2014, **97**, 3197.
11 D. P. Xu, H. Yang, L. Li, Q. Zhou, H. M. Yuan and T. Cui, *Cryst. Res. Technol.*, 2014, **49**, 502.
12 D. A. Spassky, V. N. Shlegel, N. V. Ivannikova, A. P. Yelisseyev and A. B. Belsky, *Opt. Mater.*, 2015, **42**, 430.
13 Ch. Rabbow and Hk. Müller-Buschbaum, *Z. Naturforsch., B: J. Chem. Sci.*, 1996, **51**, 343.
14 Ch. Rabbow, S. Panzer and Hk. Müller-Buschbaum, *Z. Naturforsch.*, 1998, **53b**, 517.
15 V. A. Morozov, A. Bertha, K. W. Meert, S. Van Rompaey, D. Batuk, G. T. Martinez, S. Van Aert, P. F. Smet, M. V. Raskina,

D. Poelman, A. M. Abakumov and J. Hadermann, *Chem. Mater.*, 2013, **25**, 4387.

16 H. P. Ji, Z. H. Huang, Z. G. Xia, M. S. Molokeev, V. V. Atuchin, M. H. Fang and S. F. Huang, *Inorg. Chem.*, 2014, **53**, 5129.

17 A. Yousif, V. Kumar, H. A. A. Seed Ahmed, S. Som, L. L. Noto, O. M. Ntwaeaborwa and H. C. Swart, *ECS J. Solid State Sci. Technol.*, 2014, **3**, R222.

18 B. Raveau, V. Caignaert, V. Pralong and A. Maignan, *Z. Anorg. Allg. Chem.*, 2009, **635**, 1869.

19 Md. Motin Seikh, V. Caignaert, V. Pralong and B. Raveau, *J. Phys. Chem. Solids*, 2014, **75**, 79.

20 M. Valldor and O. Breunig, *Solid State Sci.*, 2011, **13**, 831.

21 M. P. Saradhi, B. Raveau, V. Caignaert and U. V. Varadaraju, *J. Solid State Chem.*, 2010, **183**, 485.

22 P. F. Jiang, Z. X. Liu, X. R. Sun, W. L. Gao, R. H. Cong and T. Yang, *J. Solid State Chem.*, 2013, **207**, 105.

23 P. F. Jiang, W. L. Gao, R. H. Cong and T. Yang, *Dalton Trans.*, 2015, **44**, 6069.

24 J. P. Perdew, K. Burke and M. Ernzerhof, *Phys. Rev. Lett.*, 1996, **77**, 3865.

25 P. Blaha, K. Schwarz, G. K. H. Madsen, D. Kvanicka, J. Luitz, 2001 WIEN2K, An augmented plane wave plus local orbital program for calculating crystal properties, Karlheinz Schwarz; Techn. Universitat Wien, Austria. ISBN: 3-9501031-1-1-2.

26 D. Koller, F. Tran and P. Blaha, *Phys. Rev. B: Condens. Matter Mater. Phys.*, 2011, **83**, 195134.

27 X. Chen and Z. G. Xia, *Opt. Mater.*, 2013, **35**, 2736.

28 N. Yamashita, *J. Phys. Soc. Jpn.*, 1973, **35**, 1089.